

Formation of Acylsilenolates from Bis(acyl)trisilanes as the Silicon Analogues of Acylenolates

Joji Ohshita,^{*,†} Hiroyuki Kawamoto,[†] Atsutaka Kunai,[†] and Henrik Ottosson[‡]

[†]Department of Applied Chemistry, Graduate School of Engineering, Hiroshima University, Higashi-Hiroshima 739-8527, Japan, and [‡]Department of Biochemistry and Organic Chemistry, Box 576, Uppsala University, 751 23 Uppsala, Sweden

Received July 3, 2010

Summary: Reactions of bis(acyl)trisilanes with tris(trimethylsilyl)silyllithium in THF, followed by treatment of the resulting dark red solutions with alkyl halides, gave the Si-alkylated products and tetrakis(trimethylsilyl)silane, indicating the formation of lithium acylsilenolates via Si–Li exchange. Exothermic formation of lithium acylsilenolate was demonstrated by DFT calculations on a model reaction.

Introduction

Functionalized silyl anions are of importance because of their usefulness as synthetic tools for variously substituted organosilicon compounds. To date, alkoxy-,¹ amino-,² fluoro-,³ arylthio-,⁴ and boryl-substituted⁵ silyl anions have been prepared, and their chemical behaviors were explored. Previously, we found that the interaction of acyltris(trimethylsilyl)silanes with tris(trimethylsilyl)silyllithium ((Me₃Si)₃SiLi) or methyl-diphenylsilyllithium (MePh₂SiLi) in THF afforded lithium silenolates via Li–SiMe₃ exchange, as the silicon analogues of lithium enolates.⁶ The structures of the lithium silenolates were first characterized by NMR spectroscopic analysis of the reaction mixtures, which indicated that the center Si–C(O) bonds possess double-bond character, depending on the substituent at the carbonyl carbon. Thus, the NMR spectra of aryl-substituted silenolates were understood in terms of lithium silenolates rather than acylsilyllithiums, while alkyl substitution increased the sp³ character of the center silicon, increasing the contribution of acylsilyllithiums

(Scheme 1). Later on, the crystal structure of a crown ether complex of potassium *tert*-butylbis(trimethylsilyl)silenolate was determined by an X-ray diffraction study, which revealed that the potassium atom was located closer to the carbonyl oxygen (K–O = 2.846 Å) rather than to the center silicon atom (K–Si = 3.714 Å) and that the central silicon atom of the potassium silenolate was markedly pyramidal.⁷ We have also revealed through density functional theory (DFT) computations that an uncomplexed silenolate is best described by a resonance structure corresponding to an acyl-substituted silyl anion rather than by a resonance structure corresponding to an idealized silenolate.⁸ According to these calculations, a potassium ion solvated by THF molecules leaves the silenolate structure rather unaffected. Recently, Apeloig and co-workers reported the crystal structures of donor-free lithium silenolates with completely planar Si centers.⁹ Lithium silenolates react readily with several kinds of electrophiles to form substitution products,¹⁰ including bis(acyl)trisilanes from the reactions with acyl chlorides, as the first example of silicon analogues of 1,3-diones (Scheme 2).¹¹ In this paper, we report the formation of lithium acylsilenolates from bis(acyl)trisilanes, as the first example of silicon analogues of acylenolates.¹²

Results and Discussion

Formation of Lithium Acylsilenolates. When 2,2-dimesitylhexamethyltrisilane (**1a**) was treated with 1.2 equiv of (Me₃Si)₃SiLi in THF at –80 °C, the pale yellow solution immediately became dark red and tetrakis(trimethylsilyl)silane ((Me₃Si)₄Si) was formed quantitatively. After the mixture was stirred for 1 h at this temperature, alkyl halides were added to the dark red solution to produce Si-substituted products, dimesitylalkyldisilanes **2aa–2ad**, together with small amounts of 1,2-dione **3a**, as summarized in Table 1 (Scheme 2). The reaction with methyl iodide proceeded

*To whom correspondence should be addressed. Tel: +81-82-424-7743. Fax: +81-82-424-5494. E-mail: jo@hiroshima-u.ac.jp.

(1) (a) Tamao, K.; Kawachi, A. *Angew. Chem., Int. Ed. Engl.* **1995**, *34*, 818. (b) Tamao, K.; Kawachi, A. *Organometallics* **1995**, *14*, 3108. (c) Kawachi, A.; Tamao, K. *Organometallics* **1996**, *15*, 4653. (d) Kawachi, K.; Maeda, H.; Nakamura, H.; Doi, N.; Tamao, K. *J. Am. Chem. Soc.* **2001**, *123*, 3143.

(2) (a) Tamao, K.; Kawachi, A.; Ito, Y. *J. Am. Chem. Soc.* **1992**, *114*, 3989. (b) Kawachi, A.; Tamao, K. *J. Am. Chem. Soc.* **2000**, *122*, 1919. (c) Kawachi, A.; Maeda, H.; Tamao, K. *Organometallics* **2002**, *21*, 1319.

(3) Molev, G.; Bravo-Zhivotovskii, D.; Karni, M.; Tumanskii, B.; Botoshansky, M.; Apeloig, Y. *J. Am. Chem. Soc.* **2006**, *128*, 2784.

(4) Kawachi, A.; Oishi, Y.; Kataoka, T.; Tamao, K. *Organometallics* **2004**, *23*, 2949.

(5) Kajiwaru, T.; Takeda, N.; Sasamori, T.; Tokitoh, N. *Organometallics* **2008**, *27*, 880.

(6) (a) Ohshita, J.; Masaoka, Y.; Masaoka, S.; Ishikawa, M.; Tachibana, A.; Yano, T.; Yamabe, T. *J. Organomet. Chem.* **1994**, *473*, 15. (b) Ohshita, J.; Masaoka, S.; Masaoka, Y.; Hasebe, H.; Ishikawa, M.; Tachibana, A.; Yano, T.; Yamabe, T. *Organometallics* **1996**, *15*, 3136. (c) Ohshita, J.; Sakurai, H.; Tokunaga, Y.; Kunai, A. *Organometallics* **1999**, *18*, 4545. (d) Bravo-Zhivotovskii, D.; Apeloig, Y.; Ovchinnikov, Y.; Ignonin, V.; Struchkov, Y. T. *J. Organomet. Chem.* **1993**, *446*, 123.

(7) Guliasvili, T.; El-Sayed, I.; Fischer, A.; Ottosson, H. *Angew. Chem., Int. Ed.* **2003**, *42*, 1640.

(8) (a) Ottosson, H. *Chem.—Eur. J.* **2003**, *9*, 4144. (b) Eklöf, A. M.; Ottosson, H. *Tetrahedron* **2009**, *65*, 5521.

(9) Dobrovetsky, R.; Zborovsky, L.; Sheberla, D.; Botoshansky, M.; Bravo-Zhivotovsky, D.; Apeloig, Y. *Angew. Chem., Int. Ed.* **2010**, *49*, 4084.

(10) (a) Ohshita, J.; Masaoka, S.; Morimoto, Y.; Sano, M.; Ishikawa, M. *Organometallics* **1997**, *16*, 1123. (b) Ohshita, J.; Masaoka, S.; Morimoto, Y.; Ishikawa, M. *Organometallics* **1997**, *16*, 910. (c) Ohshita, J.; Tamai, M.; Sakurai, H.; Kunai, A. *Organometallics* **2001**, *20*, 1065.

(11) Ohshita, J.; Tokunaga, Y.; Sakurai, H.; Kunai, A. *J. Am. Chem. Soc.* **1999**, *121*, 6080.

(12) Preliminary results for the formation of lithium acylsilenolates have been reported. See ref 11.

cleanly, and the formation of methylated product **2aa** in high yield was confirmed by the mass and NMR spectra of the reaction mixture. However, **2aa** readily decomposed during the workup process and hence could not be separated from the mixture. With bulkier alkyl halides, many unidentified byproducts were detected in low yields in the reaction mixtures, lowering the yields of the alkylated products, in contrast to the reaction with methyl iodide. Products **2ab–2ad** were more stable than **2aa** and could be isolated, but still underwent decomposition to an extent by subjecting them to column chromatography. Similar reactions of **1b** also proceeded to give the corresponding alkylated products **2ba–2bd**, together with **3b** as a minor product. Methylated product **2ba** could not be isolated, again.

The formation of $(\text{Me}_3\text{Si})_4\text{Si}$ and alkylated products **2** clearly indicates the formation of lithium acylsilenolates by

Scheme 1. Lithium Silenolate (left) and Acylsilyllithium (right)



Scheme 2. Formation and Reactions of Lithium Acylsilenolates

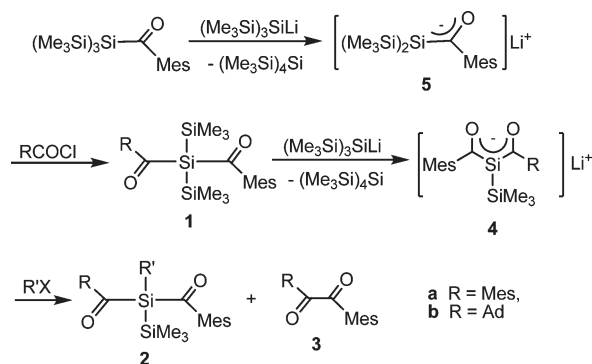
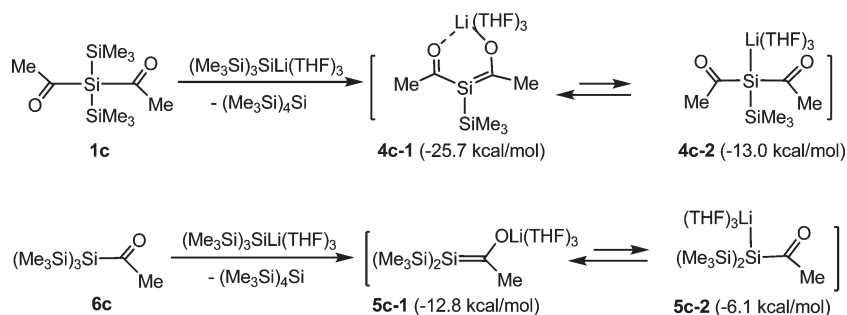


Table 1. Formation and Reactions of Lithium Acylsilenolates

R	R'X	product	yield/% ^a	
Mes (1a)	MeI	2aa	93	3a
	<i>i</i> PrI	2ab	42 (35)	
	allylBr	2ac	51 (40)	
	PhCH ₂ Br	2ad	46 (38)	
Ad (1b)	MeI	2ba	91	3b
	<i>n</i> BuBr	2bb	46 (38)	
	allylBr	2bc	48 (40)	
	PhCH ₂ Br	2bd	41 (33)	

^aYields were determined by ¹H NMR spectra of the reaction mixtures. Isolated yields are given in parentheses.

Scheme 3. Reaction Heats of Formation of Lithium Silenolates (4c** and **5c**), Derived from DFT Calculations at the B3LYP/6-31+G(d)//B3LYP/6-31G(d) Level**



Li–SiMe₃ exchange (Scheme 2). However, lithium acylsilenolates were thermally rather unstable, and standing the solutions of **4a** and **4b** overnight at $-80\text{ }^\circ\text{C}$ followed by quenching with methyl iodide led to no formation of **2aa** or **2ba**, but produced complex mixtures containing **3a** and **3b** in 38% and 31% yield, respectively. This is in marked contrast to lithium silenolate **5** reported previously (Scheme 2), which was stable even at room temperature for a few days. The route leading to **3a** and **3b** is still unclear. However, the fact that compound **3a** was not detected at all in the reaction mixtures of **1b** indicated that **3b** arose from intramolecular thermal decomposition of **4b**. We examined also the reactions of **1a** and **1b** with $(\text{Me}_3\text{Si})_3\text{SiLi}$, followed by quenching of the resulting acylsilenolates **5** with methanol. However, the reactions gave complex mixtures, from which no major products could be separated.

Computational Studies. To understand the electronic structure of lithium acylsilenolates, we carried out DFT calculations at the B3LYP/6-31+G(d)//B3LYP/6-31G(d) level on model reactions shown in Scheme 3. For all the lithium compounds examined in the computational studies, three THF molecules are coordinated to the lithium atom. Addition of one more THF molecule in the input geometries always resulted in the displacement of one of the THF molecules during the optimization. In these reactions, two kinds of stable isomers are obtained as the products, and oxylithiums **4c-1** and **5c-1** are more stable than silyllithiums **4c-2** and **5c-2**, respectively. It is also noted that the formation of **4c-1** and **4c-2** from **1c** is more exothermic than that of **5c-1** and **5c-2** from **6c**, respectively. Table 2 lists the structural parameters of **4c** and **5c** derived from the calculations, and Figure 1 represents the optimized geometries of **4c-1** and **4c-2**. Compound **4c-1** possesses a bidentate structure with slightly unsymmetrical Li–O bonding of 1.937 and 1.999 Å. Such chelation seems to be responsible for the more exothermic formation of **4c-1** than that of **5c-1**. The central Si–C(O) bonds of **4c-1** are 1.904 and 1.900 Å, in between those of **5c-1** (1.864 Å) and **4c-2** (1.947, 1.943 Å), indicating that the double-bond character of the center Si–C bonding increases in the order **4c-2** < **4c-1** < **5c-1**. The sum of the Si–C and Si–Si bond angles around the center silicon atom of **4c-1** is 324.7° , larger than those of **4c-2** (317.7°) and $(\text{Me}_3\text{Si})_3\text{SiLi}(\text{THF})_3$ (309.3°) obtained by the calculations, being also indicative of the sp^2 character of **4c-2** to an extent, although this is still in the range of sp^3 bonding and smaller than that of **5c-1** (330.7°). Molecule **4c-2** has a monodentate structure without evident Li–O interactions, similarly to **5c-2**. In fact, the C=O (1.239, 1.238 Å) and Si–C(O) (1.947, 1.943 Å) bond lengths are a little different from, but close to, those of **1c** (both 1.225 Å for C=O and 1.961,

Table 2. Structural Parameters of Lithium Acylsilenolate **4c and Silenolate **5c**, Derived from DFT Calculations^a**

compd	Si–C(=O)/Å	C=O/Å	∑(Si bond angles)/deg ^b
4c-1	1.904, 1.900	1.256, 1.254	324.7
4c-2	1.947, 1.943	1.239, 1.238	317.7
5c-1	1.864	1.281	330.7
5c-2	1.952	1.241	315.7

^a At the B3LYP/6-31+G(d)//B3LYP/6-31G(d) level. ^b Sum of Si–C and Si–Si bond angles around the center silicon atom.

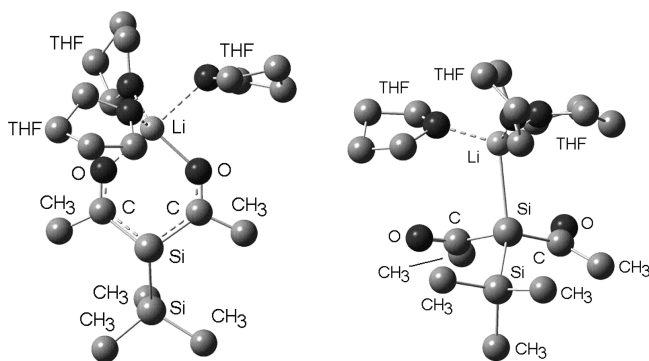


Figure 1. Optimized geometries of lithium acylsilenolates **4c-1** (left) and **4c-2** (right) derived from DFT calculations at the B3LYP/6-31G(d) level. Hydrogen atoms are omitted for clarity.

1.959 Å for Si–C(O)). It is likely, therefore, that inductive electron-withdrawing effects of the acyl groups are primarily responsible for the more exothermic formation of **4c-2** than that of **5c-2**, and no significant stabilization by extra coordination through acyl–Li interaction is involved in this compound.

In conclusion, on the basis of the results described above, we demonstrate the smooth formation of lithium acylsilenolates by the reactions of bis(acyl)trisilanes with $(\text{Me}_3\text{Si})_3\text{SiLi}$ via Li–SiMe₃ exchange. Treatment of the resulting lithium acylsilenolates with electrophiles provides a route to variously substituted bisacyldisilanes. DFT calculations on model reactions were performed, which suggested that the formation of lithium acyl silenolate is more exothermic than that of lithium silenolate, due to the extra coordination of the acyl oxygen to the lithium atom and inductive electron-withdrawing effects of the acyl groups. However, experimental observation clearly indicated that lithium acylsilenolate is thermally less stable than lithium silenolate, probably due to the intramolecular reactions leading to many decomposition products including 1,2-diones **3a** and **3b**. Studies on the reactivity of lithium acylsilenolates toward other electrophiles are under way.

Experimental Section

General Procedures. All reactions were carried out in dry nitrogen. THF and ether were distilled from sodium-benzophenone ketyl immediately before use. NMR spectra were recorded on a JEOL model LA-400 spectrometer. Low-resolution mass spectra were measured on a Shimadzu model QP-5050A spectrometer, while high-resolution mass spectra were obtained on a JEOL model SX-102A spectrometer. Compounds **1a** and **1b** were prepared as reported in the literature.¹¹

Reactions of **1a and **1b** with $(\text{Me}_3\text{Si})_3\text{SiLi}$, Followed by Alkyl Halides.** To a solution of 94 mg (0.20 mmol) of **1a** in 1.0 mL of THF was added a solution of 0.24 mmol of $(\text{Me}_3\text{Si})_3\text{SiLi}$ in 2 mL of THF/ether at -80°C . After the mixture was stirred at this

temperature for 1 h, 2.0 mmol of isopropyl iodide was added and the mixture was allowed to warm to room temperature. The mixture was hydrolyzed with water and the organic layer was separated. The organic layer was dried over anhydrous magnesium sulfate. After evaporation of the solvent, the residue was analyzed by ¹H NMR spectroscopy as being **2ab** (42% yield), **3a** (5% yield), and $(\text{Me}_3\text{Si})_4\text{Si}$ (quant). Compounds **2ab** and **3a** were isolated by preparative GPC, eluting with toluene. Data for **2ab**: MS m/z 438 (M^+); ¹H NMR (δ in C_6D_6) 0.27 (s, 9H, Me₃Si), 1.14 (d, 6H, $J = 7.22$, Me₂CH–), 1.59 (sept, 1H, $J = 6.99$ Hz, Me₂CH–), 2.02 (s, 6H, p -Me), 2.15 (s, 12H, o -Me), 6.52 (s, 4H, ring H); ¹³C NMR (δ in C_6D_6) 0.3, 15.2, 19.5, 19.7, 21.0, 129.1, 132.7, 138.3, 144.8, 245.2; exact MS calcd for $\text{C}_{26}\text{H}_{38}\text{O}_2\text{Si}_2$ (M^+) 438.2410, found 438.2398. Data for **3a**: MS m/z 147 ($\text{M}^+ - \text{COMes}$); ¹H NMR (δ in C_6D_6) 2.04 (s, 12H, o -Me), 2.15 (s, 6H, p -Me), 6.61 (s, 4H, ring H); ¹³C NMR (δ in C_6D_6) 20.2, 21.0, 129.0, 134.8, 135.7, 139.7, 198.3. Anal. Calcd for $\text{C}_{20}\text{H}_{22}\text{O}_2$: C, 81.60; H, 7.53. Found: C, 81.30; H, 7.23.

Other substitution reactions of **1a** and **1b** were carried out in a fashion similar to that above. Data for **2aa**: MS m/z 410 (M^+); ¹H NMR (δ in C_6D_6) 0.18 (s, 9H, Me₃Si), 0.48 (s, 3H, MeSi), 2.03 (s, 6H, p -CH₃), 2.11 (s, 12H, o -CH₃), 6.55 (s, 4H, ring H). Data for **2ac**: MS m/z 436 (M^+); ¹H NMR (δ in C_6D_6) 0.21 (s, 9H, Me₃Si), 2.03 (s, 6H, p -Me), 2.15 (s, 12H, o -Me), 2.17 (d, 2H, $J = 7.98$, H₂C=CHCH₂–), 4.81 (dd, 2H, $J = 13.75$, 1.44 Hz, H₂C=CHCH₂–), 5.73–5.84 (m, 1H, H₂C=CHCH₂–), 6.54 (s, 4H, ring H); ¹³C NMR (δ in C_6D_6) –0.6, 19.6, 21.0, 21.2, 115.4, 129.1, 132.7, 133.5, 138.5, 144.4, 243.8; exact MS calcd for $\text{C}_{26}\text{H}_{36}\text{O}_2\text{Si}_2$ (M^+) 436.2254, found 436.2260. Data for **2ad**: MS m/z 486 (M^+); ¹H NMR (δ in C_6D_6) 0.08 (s, 9H, Me₃Si), 2.03 (s, 6H, p -CH₃), 2.09 (s, 12H, o -CH₃), 2.77 (s, 3H, PhCH₂–), 6.55 (s, 4H, Mes ring H), 6.89–7.01 (m, 5H, Ph); ¹³C NMR (δ in C_6D_6) –0.7, 19.6, 21.0, 22.9, 125.3, 128.6, 129.1, 129.4, 132.8, 138.4, 138.6, 144.4, 244.0; exact MS calcd for $\text{C}_{30}\text{H}_{38}\text{O}_2\text{Si}_2$ (M^+) 486.2410, found 486.2409. Data for **2ba**: MS m/z 426 (M^+); ¹H NMR (δ in C_6D_6) 0.30 (s, 9H, Me₃Si), 0.83 (s, 3H, MeSi), 1.57 (br s, 6H, Ad), 1.87 (br s, 9H, Ad), 2.03 (s, 3H, p -Me), 2.18 (s, 6H, o -Me), 6.58 (s, 2H, ring H). Data for **3b**: MS m/z 468 (M^+); ¹H NMR (δ in C_6D_6) 1.76 (br s, 6H, Ad), 2.08 (br s, 6H, Ad), 2.18 (s, 6H, o -Me), 2.27 (s, 3H, p -Me), 6.83 (s, 2H, ring H). Data for **2bb**: MS m/z 468 (M^+); ¹H NMR (δ in C_6D_6) 0.30 (s, 9H, Me₃Si), 0.83 (t, 3H, $J = 7.24$, CH₃(CH₂)₃–), 1.16–1.53 (m, 6H, CH₃–(CH₂)₃–), 1.57 (br s, 6H, Ad), 1.87 (br s, 9H, Ad), 2.03 (s, 3H, p -Me), 2.18 (s, 6H, o -Me), 6.58 (s, 2H, ring H); ¹³C NMR (δ in C_6D_6) –0.2, 13.7, 14.1, 19.7, 20.9, 27.0, 27.5, 28.2, 36.7, 37.4, 52.1, 129.1, 132.4, 138.3, 145.0, 243.9, 246.1; exact MS calcd for $\text{C}_{28}\text{H}_{44}\text{O}_2\text{Si}_2$ (M^+) 468.2880, found 438.2897. Data for **2bc**: MS m/z 452 (M^+); ¹H NMR (δ in C_6D_6) 0.28 (s, 9H, Me₃Si), 1.57 (s, 6H, Ad), 1.82–1.89 (m, 9H, Ad), 2.03 (s, 3H, p -Me), 2.09 (m, 1H, H₂C=CHCH₂–), 2.13 (s, 6H, o -Me), 2.09 (ddt, 1H, $J = 13.5$, 8.1, 1.0 Hz, H₂C=CHCH₂–), 4.86 (dd, 1H, $J = 10.1$, 1.0 Hz, H₂C=), 4.92 (dd, 1H, $J = 17.1$, 1.7 Hz, CH₂=), 5.86–5.97 (m, 1H, H₂C=CHCH₂–), 6.60 (s, 2H, ring H); ¹³C NMR (δ in C_6D_6) –0.2, 19.8, 21.0, 21.4, 28.3, 36.8, 37.3, 52.1, 115.3, 129.2, 132.4, 134.2, 138.4, 144.6, 242.9, 245.1; exact MS calcd for

(13) Frisch, M. J.; Trucks, G. W.; Schlegel, H. B.; Scuseria, G. E.; Robb, M. A.; Cheeseman, J. R.; Scalmani, G.; Barone, V.; Mennucci, B.; Petersson, G. A.; Nakatsuji, H.; Caricato, M.; Li, X.; Hratchian, H. P.; Izmaylov, A. F.; Bloino, J.; Zheng, G.; Sonnenberg, J. L.; Hada, M.; Ehara, M.; Toyota, K.; Fukuda, R.; Hasegawa, J.; Ishida, M.; Nakajima, T.; Honda, Y.; Kitao, O.; Nakai, H.; Vreven, T.; Montgomery, J. A., Jr.; Peralta, J. E.; Ogliaro, F.; Bearpark, M.; Heyd, J. J.; Brothers, E.; Kudin, K. N.; Staroverov, V. N.; Kobayashi, R.; Normand, J.; Raghavachari, K.; Rendell, A.; Burant, J. C.; Iyengar, S. S.; Tomasi, J.; Cossi, M.; Rega, N.; Millam, J. M.; Klene, M.; Knox, J. E.; Cross, J. B.; Bakken, V.; Adamo, C.; Jaramillo, J.; Gomperts, R.; Stratmann, R. E.; Yazyev, O.; Austin, A. J.; Cammi, R.; Pomelli, C.; Ochterski, J. W.; Martin, R. L.; Morokuma, K.; Zakrzewski, V. G.; Voth, G. A.; Salvador, P.; Dannenberg, J. J.; Dapprich, S.; Daniels, A. D.; Farkas, O.; Foresman, J. B.; Ortiz, J. V.; Cioslowski, J.; Fox, D. J. *Gaussian 09*, Revision A.02; Gaussian, Inc.: Wallingford, CT, 2009.

$C_{27}H_{40}O_2Si_2$ (M^+) 452.2567, found 452.2556. Data for **2bd**: MS m/z 502 (M^+); 1H NMR (δ in C_6D_6) 0.14 (s, 9H, Me_3Si), 1.56 (s, 6H, Ad), 1.83–1.89 (m, 9H, Ad), 2.05 (s, 3H, *p*-Me), 2.09 (s, 6H, *o*-Me), 2.64 (d, 1H, $J = 13.75$ Hz, $PhCH_2-$), 3.06 (d, 1H, $J = 13.75$ Hz, $PhCH_2-$), 6.58 (s, 2H, Mes ring Hs), 6.90–7.07 (m, 5H, Ph); ^{13}C NMR (δ in C_6D_6) –0.1, 19.8, 21.0, 22.2, 28.3, 36.8, 37.4, 52.3, 125.2, 128.6, 129.3, 129.5, 132.7, 138.6, 139.2, 144.5, 243.1, 245.2; exact MS calcd for $C_{31}H_{42}O_2Si_2$ (M^+) 502.2723, found 502.2739.

(14) (a) Becke, A. D. *J. Chem. Phys.* **1993**, *98*, 5648. (b) Stephens, P. J.; Devlin, F. J.; Chabalovski, C. F.; Frisch, M. J. *J. Phys. Chem.* **1994**, *98*, 11623. (c) Raghavashari, K.; Binkley, J. S.; Seeger, R.; Pople, J. A. *J. Chem. Phys.* **1980**, *72*, 650.

DFT Calculations. All calculations were performed with DFT, using the Gaussian09 program package.¹³ The B3LYP hybrid density functional theory method and the 6-31G(d) basis set were employed for the geometry optimization, and the energies were obtained at the B3LYP/6-31+G(d) level.¹⁴

Acknowledgment. Financial support from Shorai Foundation for Science and Technology and the Swedish Research Council is gratefully acknowledged.

Supporting Information Available: Cartesian coordinates for optimized geometries of all the calculated model compounds. This material is available free of charge via the Internet at <http://pubs.acs.org>.